cannot occur in the symmetric fashion available to the vicinal diols, due to the presence of at least one aldehyde or carboxylate group. One can envisage electrooxidation of such unsymmetrical reactants involving surface bonding of only one functional group.

It is interesting to compare the selective electrocatalytic properties of nickel with platinum. While the latter catalyst provides an efficient exhaustive electrooxidation of ethylene glycol and glycerol (i.e., yielding carbonate), it lacks the high degree of selectivity displayed by nickel in that comparable amounts of the exhaustive C_2 oxidation product, oxalate, are commonly formed (Figure 5). A further difference is that nickel yields selectively the *partial* oxidation product, formate. Comparison of the product distributions for electrooxidation of glycolate, glyoxal, and glyoxylate also highlights a higher efficiency of C–C bond cleavage exhibited by nickel in comparison with platinum but in somewhat different fashion. Thus electrooxidation of these C_2 species on nickel yields chiefly carbonate, with little or no oxalate formed alongside, whereas the opposite product distribution is observed on platinum.

This greater ability of the nickel surface to incur oxidative C–C bond cleavage may arise from the electropositive nature of the nickel sites and the consequent withdrawal of electron density from the carbon atoms. Whereas the nickel surface consists of a thick oxide film, the platinum surface is largely unoxidized in the potential region, −0.6 to −0.2 V, where the organic oxidative chemistry of concern here is occurring. [The latter circumstance can readily be deduced by inspecting the cyclic voltammogram (dotted curve) for Pt in 0.5 M KOH alone in Figure 1B.] Such reduced Pt surface sites can readily cleave C–H bonds, forming adsorbed hydrogen atoms, thereby providing electrooxidative pathways where the C_2 moiety remains at least partly intact, as in the production of oxalate. This property of platinum surfaces is also reflected in the facile electrooxidation of formate ($HCOO^-$) to carbonate on this metal, a process which does not occur on nickel and gold.

The present findings provide clear evidence of the virtues of real-time infrared spectroscopy for deducing in quantitative fashion detailed reaction pathways for electrocatalytic organic processes. Some marked, and in some respects unexpected, differences in the nature of the catalytic pathways for ethylene glycol electrooxidation on gold, platinum, and nickel surfaces are uncovered by these results. While gold provides pathways featuring sequential partially oxidized solution-phase intermediates, both platinum and nickel yield highly oxidized solution-phase products that are much more specific to the initial reactant. The remarkable ability of the nickel surface to incur highly selective C–C bond cleavage is intriguing and deserves future attention. Further studies of organic electrocatalysis utilizing real-time infrared spectroscopy, emphasizing ordered monocrystalline surfaces, are currently being pursued in our laboratory.

Acknowledgment. This work is supported by the National Science Foundation and the Office of Naval Research.

Registry No. $HO(CH_2)_2OH$, 107-21-1; Au, 7440-57-5; Pt, 7440-06-4; Ni, 7440-02-0; CO_3^{2-}, 3812-32-6; HCO_2^-, 71-47-6; $H_3CCO_2^-$, 71-50-1; OHCCHO, 107-22-2; $HOCH_2CO_2^-$, 57122-18-6; $HC(O)CO_2^-$, 430-75-1; $^-O_2CCO_2^-$, 338-70-5; KOH, 1310-58-3; $H_3CCH(OH)CH(OH)CH_3$, 513-85-9; $H_3CCH(OH)CH_2OH$, 57-55-6.

Characterization of the Ligand Environment of Vanadyl Complexes of Apoferritin by Multifrequency Electron Spin-Echo Envelope Modulation

Gary J. Gerfen,[†,‡] Phillip M. Hanna,[§,⊥] N. Dennis Chasteen,*[,§] and David J. Singel*[,†]

Contribution from the Departments of Chemistry, Harvard University, Cambridge, Massachusetts 02138, and University of New Hampshire, Durham, New Hampshire 03824. *Received February 6, 1991*

Abstract: The nature of the Fe^{2+} and Fe^{3+} binding sites on the protein shell of ferritin and their role in the accumulation of iron within this storage protein are poorly understood. An ESEEM (electron spin-echo envelope modulation) study is reported which provides new insight into the nature of these sites in the horse spleen protein. ESEEM spectra have been obtained of complexes of horse spleen apoferritin with VO^{2+}—an ion that binds apoferritin competitively with both Fe^{2+} and Fe^{3+}; samples prepared both in ^1H_2O and ^2H_2O and at both pH ~5.5 and at ~7.4, which correspond respectively to the α and β species of Chasteen and Theil (*J. Biol. Chem.* **1982**, *257*, 7672-7677), have been studied. The ESEEM spectra clearly reveal the presence of endogenous nitrogen in the environment of VO^{2+} in both types of complexes. This nitrogen most likely derives from an imidazole ligand of a histidine residue coordinated cis to the vanadyl oxo group. ESEEM is also observed from a proton whose dipolar coupling to the VO^{2+} center is characteristic of a hydrogen attached to the coordinated atom of a cis ligand. This hydrogen undergoes exchange with aqueous solvent; the VO^{2+} binding site is thus solvent-accessible. The ratio of the amplitude of the ESEEM peak associated with this proton in the β vs the α complex is approximately 0.5. Attribution of these ESEEM features to the hydrogens of a cis-coordinated aquo ligand that deprotonates to hydroxide at pH ≈6.5 is consistent with these observations. The ESEEM results are best interpreted in terms of a binding site that accommodates VO^{2+} with one aquo and one histidine ligand—and with other coordination positions filled by protein carboxylate donors. The possible location of this VO^{2+} binding site and its significance to iron accumulation in ferritin are discussed.

I. Introduction

Ferritins are proteins that store iron as a hydrous ferric oxide mineral core of ~80-Å diameter within a highly symmetrical assembly of 24 ~20-kDa subunit proteins.[1] In recent years, numerous studies have been undertaken to develop an understanding of the detailed process through which this storage takes place—in particular to elucidate the role played by the protein coat in the sequestration and oxidation of ferrous iron, the hy-

[†] Harvard University.
[‡] Present address: Francis Bitter National Magnet Laboratory, Massachusetts Institute of Technology, Cambridge, MA 02139.
[§] University of New Hampshire.
[⊥] Present address: National Institute of Environmental Health Sciences, P.O. Box 12233, Research Triangle Park, NC 27709.

(1) (a) Crichton, R. R. *Struct. Bonding* **1973**, *17*, 66. (b) Bourne, P. E.; Harrison, P. M.; Lewis, W. G.; Rice, D. W.; Smith, J. M. A.; Stansfield, R. F. D. In *The Biochemistry and Physiology of Iron*; Saltman, P., Heganauer, J., Eds.; Elsevier/North-Holland Biomedical: Amsterdam, 1982; p 345. (c) Crichton, R. R.; Charloteaux-Wauters, M. *Eur. J. Bioch.* **1987**, *164*, 485. (d) Theil, E. C. *Annu. Rev. Biochem.* **1987**, *56*, 289. (e) Theil, E. C. *Adv. Enzymol. Relat. Areas Mol. Biol.* **1989**, *63*, 421.

0002-7863/91/1513-9513$02.50/0

drolysis of ferric iron, and the nucleation and growth of the polymeric oxide core.[2-11]

EPR (electron paramagnetic resonance) of the spin probe[12,13] vanadyl ion, VO^{2+}, has been fruitfully employed to study the initial stages of this process—specifically, the interaction of metal ions with the metal-free protein apoferritin.[4-6] The binding stoichiometry of the first-formed VO^{2+}–apoferritin complex (one VO^{2+} per three protein subunits) has been determined, and the displacement of VO^{2+} from the protein by both Fe^{2+} and Fe^{3+} during very early stages of iron deposition as well as by Cd^{2+} and Tb^{3+}—both of which are known to inhibit core formation[11]—has been demonstrated.[4-6]

Numerous metal ion binding sites in the apoprotein have been identified by X-ray crystallography,[14] but their role, if any, in the mechanism of iron deposition has not been elucidated. The stoichiometry of the initially formed apoferritin complex with VO^{2+} suggests that its principal binding sites are associated with the eight hydrophilic channels that pass through the protein coat, at each interface of three protein subunits related by a 3-fold symmetry axis. Further insight into the nature of the VO^{2+} binding sites can be drawn from spectroscopic data obtained in EPR studies of the VO^{2+}–apoferritin complex. The electron g factors and ^{51}V hyperfine coupling parameters[5] are consistent—both on the basis of specific precedents and more generally on ligand "additivity relationships"[13]—with VO^{2+} in an environment in which the ligands are, to name two possibilities, carboxylates or a combination of carboxylate, N donor, and aquo ligands.

An intriguing observation in the EPR experiments[5] involves the dependence of the spectral features and parameters on the pH of the sample. At pH ~5.4, the EPR spectrum is dominated by a species referred to as "α". As the pH is raised, the intensity of the α spectrum decreases, while a new species, "β", emerges. At pH ~7.5 the EPR spectrum is dominated by the β species. Aside from the distinct α and β spectra no other EPR substructures indicative of additional, spectroscopically distinct binding sites are observed. The pH-dependent interconversion of the α and β species presumably reflects a deprotonation of some functional group in the vicinity of the EPR spin probe, possibly a vanadyl-coordinated solvent ligand.[4,5]

Unfortunately, the EPR spectra do not provide *direct* evidence concerning the identity of the VO^{2+} ligands. Inasmuch as the unpaired electron spin density in VO^{2+} complexes tends to be localized in a vanadium-centered, nonbonding orbital, hyperfine structure from ligand nuclei—which could provide insight into their identity—is generally not resolved in VO^{2+} EPR powder patterns.[13] The ESEEM (electron spin-echo envelope modulation) technique[15,16] provides a means to circumvent limitations imposed by EPR resolution in tapping the information carried by the nuclear spin interactions. The spectra of nuclear spins in the vicinity of the paramagnetic probe can be obtained by spectral analysis of nuclear modulation effects manifest in ESEEM patterns—recordings of the amplitude of an electron spin echo as the time between pulses employed in its generation is incremented.

In this paper we report an ESEEM study of VO^{2+} complexes of horse spleen apoferritin that provides new insight into the nature of the metal site. Spectroscopic strategies involving orientation-selective excitation[17,18] and tracking of external field dependences[19-25] of the ESEEM spectral features are employed in the study. The combinations of the fundamental nuclear spin frequencies that appear in two-pulse ESEEM spectra[16] are also of special utility in the work presented here: They provide a simple route toward the removal of line broadening that arises in ESEEM powder patterns because of the anisotropy of certain nuclear spin interactions. These line-narrowing effects facilitate the observation, assignment, and analysis of spectral features. The ESEEM results indicate the presence of a nitrogen—most likely from a coordinated imidazole of a histidine residue—in the coordination sphere of VO^{2+} cis to the oxo group. An ESEEM peak from strongly coupled, H_2O-exchangeable protons is also observed; the intensity of this peak for the α species is approximately twice that observed for the β. Our results are consistent with the presence of a cis aquo ligand which deprotonates to hydroxide near neutral pH. The possible location and functional significance of this metal ion binding site in the apoferritin molecule are discussed.

II. Experimental Methods

Materials. Horse spleen ferritin (3× crystallized, cadmium free) was purchased from Boehringer Mannheim Biochemicals. All chemicals used were reagent grade or better and were used without further purification. MES (2-*N*-morpholinoethanesulfonic acid) and HEPES (*N*-(2-hydroxyethyl)-piperazine-*N'*-2-ethanesulfonic acid) buffers were purchased from Research Organics Inc.; 95% thioglycolic acid, sodium chloride, and 99.999% (Gold Label) vanadyl sulfate trihydrate were from Aldrich; and Chelex Resin (dry mesh 50–100) was from Sigma Chemical Co. All deuterated chemicals (^2H_2O, $^2H_2SO_4$, ^2HCl, NaO^2H) were purchased from Stohler Isotope Chemicals (Waltham, MA).

Sample Preparation. Apoferritin was prepared using thioglycolic acid as described previously.[5] Eight equivalents of vanadyl ion (from an aqueous solution 0.05 M in $VOSO_4$ and 0.1 M in H_2SO_4) per protein was added in the absence of dioxygen to a solution ~0.1–0.2 mM in apoferritin, 0.1 M in NaCl, and either 0.15 M in MES (pH 5–6) or 0.15 M in HEPES (pH 7–8) buffers. Before the vanadyl ion addition, the apoferritin solutions were deoxygenated by purging with argon gas from which trace oxygen had been removed by passing it through a solution of V^{2+} in H_2SO_4 over Zn/Hg amalgam. The deuterated samples were prepared by ultrafiltration of the apoprotein solution described above

(2) Rosenberg, L. P.; Chasteen, N. D. In *The Biochemistry and Physiology of Iron*; Saltman, P., Heganauer, J., Eds.; Elsevier/North-Holland Biomedical: Amsterdam, 1982; p 405.
(3) Chasteen, N. D.; Antanaitis, B. C.; Aisen, P. *J. Biol. Chem.* **1985**, *260*, 2926.
(4) Wardeska, J. G.; Viglione, B.; Chasteen, N. D. *J. Biol. Chem.* **1986**, *261*, 6677.
(5) Chasteen, N. D.; Theil, E. C. *J. Biol. Chem.* **1982**, *257*, 7672.
(6) Hanna. P. M.: Chasteen, N. D.; Rottman, G. A.; Aisen, P. *Biochemistry* **1991**, *30*, 9210.
(7) Yang, C. Y.; Meagher, A.; Huynh, B. H.; Sayers, D. E.; Theil, E. C. *Biochemistry* **1989**, *26*, 497.
(8) Jacobs, D.; Watt, G. D.; Frankel, R. B.; Papaefthymiou, G. C. *Biochemistry* **1989**, *28*, 9216.
(9) Watt, G. D.; Frankel, R. B.; Papaefthymiou, G. C. *Proc. Natl. Acad. Sci. U.S.A.* **1985**, *82*, 3640.
(10) Lawson, D. M.; Treffry, A.; Artymiuk, P. J.; Harrison, P.; Yewdall, S. J.; Luzzago, A.; Cesareni, G.; Levi, S.; Arosio, P. *FEBS Lett.* **1989**, *254*, 207.
(11) Clegg, G. A.; Fitton, J. E.; Harrison, P. M.; Treffry, A. *Prog. Biophys. Mol. Biol.* **1980**, *36*, 53.
(12) Chasteen, N. D. *Struct. Bonding* **1983**, *53*, 10.
(13) Chasteen, N. D. In *Biological Magnetic Resonance*; Berliner, L. J., Reuben, J., Eds.; Plenum: New York, 1981; Vol. 3, p 3.
(14) (a) Harrison, P. M.; Ford, G. C.; Rice, D. W.; Smith, J. M. A.; Treffry, A.; White, J. L. In *Frontiers in Bioinorganic Chemistry*; Xavier, A., Ed.; VCH: Weinheim, FRG, 1986; p 268. (b) Rice, D. W.; Ford, G. C.; White, J. L.; Smith, J. M. A.; Harrison, P. M. In *Advances in Inorganic Biochemistry*; Theil, E. C., Ed.; Elsevier: New York, 1983; Vol. 5, p 39.
(15) (a) Rowan, L. G.; Hahn, E. L.; Mims, W. B. *Phys. Rev. A* **1965**, *137*, 61. (b) Mims, W. B. In *Electron Paramagnetic Resonance*; Geschwind, S., Ed.; Plenum: New York, 1972; p 263. (c) Mims, W. B.; Peisach, J. In *Biological Magnetic Resonance*; Berliner, L. J., Reuben, J., Eds.; Plenum: New York, 1981; Vol. 3, p 213. (d) Tsvetkov, Yu. D.; Dikanov, S. A In *Metal Ions in Biological Systems*; Sigel, H., Ed.; Dekker: New York, 1987; Vol. 22, p 207.
(16) Mims, W. B. *Phys. Rev. B* **1972**, *5*, 2409; **1972**, *6*, 3543.
(17) (a) Hoffman, B. M.; Martinsen, J.; Venters, R. A. *J. Magn. Reson.* **1984**, *59*, 110. (b) Hoffman, B. M.; Venters, R. A.; Martinsen, J. *Ibid.* **1985**, *62*, 537. (c) Henderson, T. A.; Kreilick, R. W. *J. Am. Chem. Soc.* **1985**, *107*, 7294. (d) Henderson, T. A.; Hurst, G. C.; Kreilick, R. W. *Ibid.* **1985**, *107*, 7299.
(18) Flanagan, H. L.; Gerfen, G. J.; Lai, A.; Singel, D. J. *J. Chem. Phys.* **1988**, *88*, 2162.
(19) Singel, D. J. In *Advanced EPR: Applications in Biology and Biochemistry*; Hoff, A. J., Ed.; Elsevier: Amsterdam, 1989; p 119.
(20) (a) Flanagan, H. L.; Singel, D. J. *J. Chem. Phys.* **1987**, *87*, 5606. (b) Flanagan, H. L.; Singel, D. J. *J. Chem. Phys.* **1988**, *89*, 2585.
(21) Lai, A.; Flanagan, H. L.; Singel, D. J. *J. Chem. Phys.* **1988**, *89*, 7161.
(22) (a) Flanagan, H. L.; Singel, D. J. *Chem. Phys. Lett.* **1987**, *137*, 391. (b) Flanagan, H. L.; Gerfen, G. J.; Singel, D. J. *J. Chem. Phys.* **1988**, *88*, 20. (c) Cosgrove, S. A.; Singel, D. J. *J. Phys. Chem.* **1990**, *94*, 2619.
(23) Cosgrove, S. A.; Singel, D. J. *J. Phys. Chem.* **1990**, *94*, 8393.
(24) Gerfen, G. J.; Singel, D. J. *J. Chem. Phys.* **1990**, *93*, 4571.
(25) Gerfen, G. J. The Magnetic Field Dependence of Electron Spin Echo Envelope Modulation. Ph.D. Thesis, Harvard University, 1990.

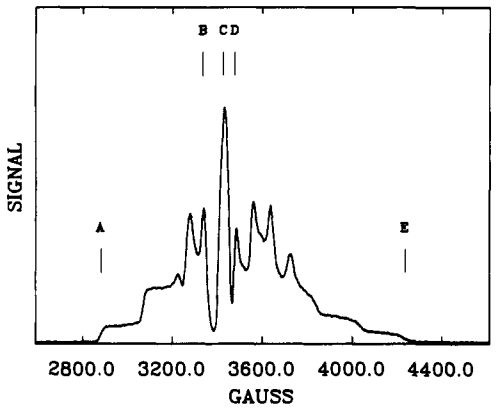

Figure 1. Electron spin-echo-detected, 9.63-GHz EPR spectrum of a VO^{2+}–apoferritin complex at 4.2 K. The sample is an α complex, pH 5.7, in ^1H_2O with a VO^{2+} concentration of 1.17 mM and a protein subunit concentration of 3.50 mM.

against ^2H_2O solutions of the appropriate buffer using an Amicon cell with a YM100 membrane, followed by addition of a vanadyl ion solution in ^2H_2O that was ~0.1 M $^2H_2SO_4$. The pH of each of the samples was adjusted by addition of sodium hydroxide or hydrochloric acid of appropriate isotopic composition. Samples were transferred via a gas-tight syringe to EPR tubes (4-mm o.d., 3-mm i.d. fused silica) purged of oxygen by a flow of purified argon. The samples were frozen and stored in dry ice.

Spectroscopy. Continuous-wave (CW) EPR spectra were obtained either at New Hampshire, on a Varian E4 spectrometer interfaced with a MINC 11/23 computer (Digital Equipment Corp.), or at Harvard with a Varian E109 spectrometer interfaced through a Stanford Research Systems module (SR245) to an IBM PC. The CW EPR spectra were obtained with sample temperatures of 77–110 K.

Electron spin echoes were generated with a spectrometer similar to that described previously.[22-25] Tunable, three-loop two-gap microwave resonators[26] were used in all of the spin-echo studies presented here; a total of three resonators were used to obtain electron spin echoes over the range of excitation frequencies spanned in the present work—8.0–11.8 GHz. The quality factor of the resonators varied from 150 to 400; the typical duration of a $\pi/2$ pulse, with an incident power of ~200 W, was 15 ns. All spin-echo spectroscopy was carried out with the sample immersed in liquid helium.

Echo-detected EPR spectra were registered at each microwave frequency surveyed. These spectra were employed in the manner described elsewhere to coordinate orientation-selective excitation in the ESEEM experiments.[25] At each EPR frequency ESEEM patterns were obtained at five different positions within the EPR line (vide infra). The α complex in ^1H_2O was investigated in greatest detail; ESEEM patterns were obtained at seven different microwave frequencies in the range 8.0–11.8 GHz. The corresponding β complex was examined at five microwave frequencies from 8.0 to 11.5 GHz. The ^2H_2O samples of both complexes were examined at 8.7 and 9.7 GHz. We primarily employed two-pulse echoes in generating the ESEEM patterns. Typical patterns consist of an average of 5–10 scans of either 256 or 512 time-domain steps of appropriate size to avoid aliasing the highest frequency peak (free-proton Larmor frequency or its first overtone). At each step, 300–10000 echoes—with single-shot signal to noise ratios of between 2 and 25 (depending on the excitation position within the EPR line)—were averaged, at a repetition rate of typically 100 Hz.

The spectral analysis of the ESEEM patterns was carried out with Fourier transformation procedures similar to those used by us previously.[22-24] Either a Gaussian or Lorentzian decay was fit to each ESEEM pattern and then subtracted from the experimental time domain prior to transformation. We mitigated dead-time artifacts by preprocessing the time-domain patterns either simply by tapering the ESEEM pattern with an extended cosine-bell function[27] or by reconstructing the time domain, by means of a linear prediction routine,[28] and then attaching the dead-time portion of the reconstruction to the experimental pattern.

III. Results and Analysis

EPR Spectroscopy. The echo-detected, 9.63-GHz EPR spectrum of the α complex of VO^{2+} and apoferritin in ^1H_2O is shown in Figure 1. The gross features of this particular spectrum as well as others obtained at different microwave frequencies are typical of vanadyl complexes.[12,13] While the electron **g** matrix shows little anisotropy, the large, anisotropic coupling between the unpaired ($3d^1$) electron and the $I = {}^7/_2$ ^{51}V nuclear spin imparts considerable structure to the spectrum. The isotropic hyperfine coupling effects an 8-fold splitting of the spectrum; the anisotropy (axial) of this coupling leads, in the orientationally disordered solid, to a spectrum comprised of eight overlapping powder patterns, with well-defined features associated with the edges of each of these eight constituent patterns.

The VO^{2+} centers in apoferritin, like most VO^{2+} complexes, possess a number of EPR properties that make them well suited to the ESEEM experiments reported here. The couniaxiality of the electron **g** and ^{51}V hyperfine interaction (^{51}**A**) matrices, together with the scant g anisotropy, facilitate the analysis of the ESEEM frequencies and their external field dependences.[24] The ^{51}V hyperfine coupling is large enough to enable the surveillance of the external field dependences of the ESEEM spectra by "field-sampling",[24] and the anisotropy of the coupling enables the performance of orientation-selective ESEEM experiments.[17,18,24] Irradiation at the positions marked A and E in the EPR spectrum of Figure 1 excites those molecules in the frozen solution that are oriented such that the major axes of their **g** and ^{51}**A** matrices are approximately parallel (within $\sim\pi/12$) to the external magnetic field; we refer to excitation at positions A and E as *parallel* excitation. At positions B–D those molecules whose unique axes are approximately orthogonal to the external field are excited; we refer to excitation at these positions as *perpendicular* excitation.

H ESEEM Spectroscopy. As noted in the Introduction, the pH-dependent change of the VO^{2+}–apoferritin EPR spectrum may stem from the deprotonation of a coordinated ligand, specifically a solvent molecule.[5] The single-crystal, proton ENDOR (electron–nuclear double resonance) study of a pentaaquovanadyl species by Atherton and Shackleton[29] provides a point of reference for anticipating the sizes of hyperfine interactions sustained by a proton attached to a vanadyl-coordinated atom—in particular to oxygen in an aquo ligand. These workers found that the isotropic hyperfine interaction, A_0^0, is nearly zero for protons of the water trans to the oxo group, but that it ranges from ~0 to 9 MHz for protons of the cis aquo ligands, depending on the orientation of the ligand about the vanadium to ligand oxygen bond. The traceless portion of the interactions was found to be nearly axially symmetric for all protons with values of the relevant coupling constant, A_2^0, of about 3.3 MHz (trans) or 4.2–5.0 MHz (cis). The observed values of A_2^0 as well as the orientations of the major axes of the proton hyperfine interaction matrices are well described as dipolar interactions between electron and proton point magnetic dipoles located at the vanadium and proton positions, respectively. These observations are reinforced in a number of other ENDOR studies of VO^{2+} complexes in single crystals and in orientationally disordered solids.[30-32]

Dipolar couplings of 3–5 MHz might appear to present some difficulty for observation in ESEEM experiments. The amplitudes of the fundamental frequency peaks, necessarily[16,21] modest in these X-band experiments, are squandered over a ^1H spectral width of ca. 5–7 MHz. This width implies, moreover, a damping of these modulation components so abrupt that little modulation depth would survive our experimental dead time of 180 ns. Recently, it has been pointed out by Schweiger[33] and by Dikanov and Astashkin[34] that the frequency dispersion of these constituent

(26) Wood, R. L.; Froncisz, W.; Hyde, J. S. *J. Magn. Reson.* **1982**, *58*, 243.
(27) Merks, R. P. J.; de Beer, R. *J. Magn. Reson.* **1980**, *37*, 30.
(28) (a) Barkhuijsen, H.; de Beer, R.; Bovee, W. M. M. J.; van Ormondt, D. *J. Magn. Reson.* **1985**, *61*, 465. (b) de Beer, R.; van Ormondt, D. In *Advanced EPR: Applications in Biology and Biochemistry*; Hoff, A. J., Ed.; Elsevier: Amsterdam, 1989; p 135.
(29) Atherton, N. M.; Shackleton, J. F. *Mol. Phys.* **1980**, *39*, 1471.
(30) van Willigen, H. *J. Magn. Reson.* **1980**, *39*, 37.
(31) Mustafi, D.; Makinen, M. W. *Inorg. Chem.* **1988**, *27*, 3360.
(32) Schweiger, A. *Struct. Bonding* **1982**, *51*, 1 and references therein.
(33) Schweiger, A. In *Advanced EPR: Applications in Biology and Biochemistry*; Hoff, A. J., Ed.; Elsevier: Amsterdam, 1989; p 243.
(34) Dikanov, S. A.; Astashkin, A. V. In *Advanced EPR: Applications in Biology and Biochemistry*; Hoff, A. J., Ed.; Elsevier: Amsterdam, 1989; p 59.

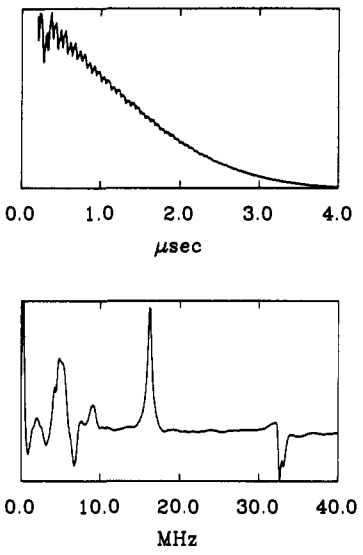

Figure 2. Two-pulse ESEEM pattern (top) and corresponding spectrum (bottom) of the VO^{2+}–apoferritin sample described in Figure 1, at 4.2 K. The modulation pattern was obtained with 10.98-GHz microwave excitation at the EPR field position marked D in Figure 1.

fundamentals is canceled in their sum-combination peak[35] and that the frequency of the consequently narrowed peak is shifted slightly above $2\nu_p$ (ν_p, the free-proton Larmor frequency). Provided that the Zeeman interaction is far greater in absolute value than the hyperfine interaction, the shift, in the absence of orientation-selective excitation (and extraneous broadening effects), may be expressed approximately, following Dikanov and Astashkin,[34]

$$\Delta\nu = A_2^{02}/2\nu_p \qquad (1)$$

An ESEEM spectrum of the VO^{2+}–apoferritin α complex obtained with 10.98-GHz excitation at position D in the EPR spectrum, that is, with perpendicular excitation, is shown in Figure 2. Proton modulation components appear at frequencies above 15 MHz. A number of additional spectral features at lower frequencies are also apparent. These modulations are assigned to ^{14}N (vide infra). The single peak at 16.3 MHz (ν_p) corresponds to the overlapping pairs of fundamental-frequency components of protons that sustain hyperfine interactions that are too small to appreciably affect their ESEEM frequencies. At $\sim 2\nu_p$, a combination peak[36] is evident; this region of the spectrum (and of two related spectra (vide infra)) is shown in greater detail in Figure 3. The observed combination peak is split into two components: The lower frequency component, located precisely at 32.6 MHz, corresponds to the combinations of the fundamentals of protons whose frequencies are not affected by hyperfine interactions; the additional structure, at the slightly higher frequency of 33.1 MHz, stems from protons coupled sufficiently strongly to sustain the shift of ~0.5 MHz that resolves their sum-combination modulation peak from the peak at $2\nu_p$. This assignment is corroborated by the external field dependence of the frequency shift, which we observe to vary linearly with the inverse of ν_p. From these measurements we evaluate $(2\nu_p\Delta\nu)^{1/2}$ to be 4.34 (0.05) MHz.[37] The partner fundamentals that correspond to this sum combination do not appear in the ESEEM spectrum: A dipolar coupling of this size would effectively preclude their observation. We also note that no other peaks are resolved in the neighborhood of $2\nu_p$ at any of the surveyed microwave frequencies and that—as illustrated in Figure 3—we observed no shifted peak (nor additional fundamental peaks) in the case of parallel excitation (EPR position A).

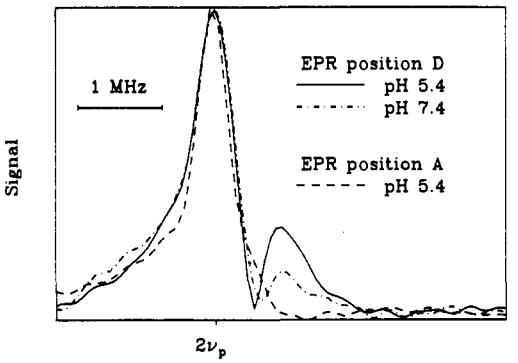

Figure 3. Proton sum-combination region of two-pulse ESEEM spectra of vanadyl–apoferritin complexes in ^1H_2O obtained at 4.2 K: (a, solid curve) an α complex (pH 5.4) with microwave excitation at field position D (Figure 1) and 9.634 GHz; (b, dot-dashed curve) a β complex (pH 7.4) with microwave excitation at field position D and 9.725 GHz; (c, dashed curve) an α complex (pH 5.4) with microwave excitation at field position A and 11.635 GHz. In all samples, the VO^{2+} concentration is 1.2 mM and the protein subunit concentration is 3.6 mM. The differences in the EPR conditions lead to small differences in the actual values of $2\nu_p$ for each spectrum shown (29.56, 29.88, and 30.87 MHz for spectra a–c, respectively). The horizontal axes of the individual spectra are shifted to compensate for the frequency offsets. The vertical axes are individually scaled to overlay the peaks that occur precisely at $2\nu_p$. The heights of these peaks are essentially identical, without rescaling, in the spectra obtained with the excitation at position D. The orientional dependence of the amplitude of the ESEEM sum-combination peak, specifically the absence of the peak in the case of parallel excitation, is seen by comparison of spectra a and c; comparison of spectra a and b reveals the pH-dependent change in the amplitude of the sum-combination peak.

Although neglected in equation 1, both the value of A_0^0 and the orientation selectivity of the EPR excitation (which restricts the range of orientations included in the powder average) exert some influence on the sum-combination frequency shift. Consideration of both effects, as briefly detailed in the Appendix, leads to the conclusion that the shifted peak derives from protons attached to the coordinated atom of a cis ligand, with a V–H distance of ~2.6 Å.

The amplitude of the peak is largely determined by the value of A_2^0 and the number of contributing nuclei.[15,16] Since A_2^0 is determined (within the systematic limits discussed in the Appendix) by the sum-combination shift, the amplitude quantifies the number of nuclei. From the amplitudes in the experimental ESEEM spectra, we surmise from detailed simulations that one to two protons contribute to this signal.[38]

A comparison is included in Figure 3 of the $2\nu_p$ region of ESEEM spectra—obtained with perpendicular excitation (EPR position D)—of the α and the β forms of the VO^{2+} apoferritin complex in ^1H_2O. The amplitude of the proton sum-combination signal at $2\nu_p$ is essentially the same in the two complexes, but the shifted peak exhibits a decline in amplitude of roughly 50%. The size of the shift, however, does not change. (We tracked the external field dependence of this shift for the β complex in a manner analogous to that described above for the α complex and determine a value of 4.25 (0.05) MHz for the quantity $(2\nu_p\Delta\nu)^{1/2}$. This value is not substantially different from that of the α complex, indicating little change in V–H distance.) Inasmuch as the sum-combination shifts are essentially the same in the α and β complexes, the loss of ESEEM intensity that accompanies the transformation of the α complex to the β must derive from a decrease—presumably from two to one—in the number of protons contributing to the signal.

An 8.74-GHz ESEEM spectrum (perpendicular excitation at position B) of an α complex of VO^{2+} with apoferritin in ^2H_2O

(35) The cancellation occurs outside the match range[21] in the *sum* combination provided $\nu_p > |A_0^0/2|$.

(36) In the cosine Fourier transforms shown, the phase of the combination peaks is opposite to that of the fundamentals as discussed in ref 16.

(37) The standard deviation in parentheses is propagated from the standard error in the slope of the least-squares best fit line obtained from a plot of the sum-combination peak shift vs ν_p^{-1} or, in tracking the ^{14}N double-quantum peak frequency (ν_{dq}), a plot of $\nu_{dq}^2/4 - \nu_n^2$ vs ν_n in which ν_n is the free ^{14}N nuclear Larmor frequency.

(38) In making this estimate, we take into account the effect that the value of A_0^0, estimated to lie in the range 0–9 MHz,[29] has on the modulation amplitudes.

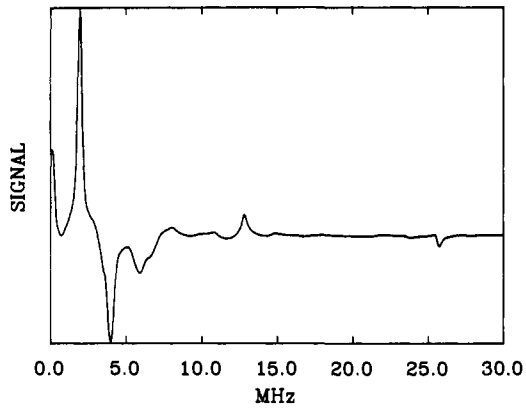

Figure 4. Two-pulse ESEEM spectrum at 8.74 GHz and magnetic field position B (Figure 1) of a VO^{2+}–apoferritin complex in ^2H_2O at 4.2 K. The sample is an α complex, 4.60 mM in protein subunits and 1.53 mM in VO^{2+}.

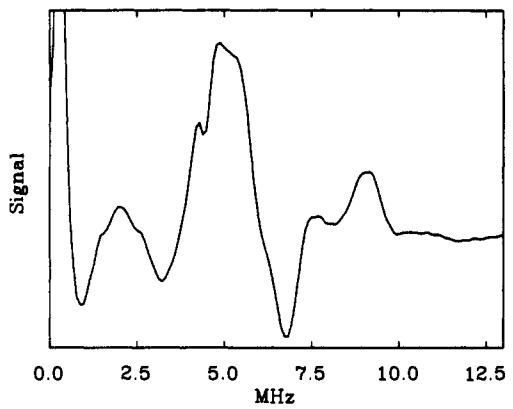

Figure 5. Expanded view of the ^{14}N region of the ESEEM spectrum of the VO^{2+}–apoferritin α complex shown in Figure 2.

is shown in Figure 4. In this spectrum, the modulation components at the proton Larmor frequency 12.8 MHz and its second harmonic are greatly reduced in amplitude as compared to those in Figure 2. They are replaced by large peaks at the deuterium Larmor frequency (1.95 MHz) and its second and third harmonic; these are intense enough to mask the other low-frequency components observed in the samples prepared in ^1H_2O. The proton sum-combination frequency component that is shifted above $2\nu_p$—which arises from the more strongly coupled protons—has vanished entirely; it does not appear in any of the spectra of complexes prepared in ^2H_2O (α or β) at any excitation frequency or any EPR irradiation position. Evidently these protons, as well as many of the very weakly coupled protons in the vicinity of the VO^{2+} probe, are accessible to solvent and undergo hydrogen exchange.

The spectrum that we obtain for the β complex in ^2H_2O differs from that shown for the α complex by a *slight* but noticeable reduction in the depth of the ^2H modulation. We surmise that the *major* contribution to signals at the ^2H Larmor frequency and its harmonics derives not from the strongly coupled hydrogens of the cis ligands but from other nearby nuclei. This situation effectively prevents us from cross-checking our quantification of the proton ESEEM results through simulation of the deuterium spectrum.[39] We observed no splittings or structure on the fundamental ^2H peaks in the spectra of either the α or the β complex. It is tempting to conclude from the absence of such splittings that none of the hydrogens that contribute significantly to the ^2H ESEEM sustain a large isotropic hyperfine interaction. The ^2H peaks at the deuterium Larmor frequency are rather broad, however, and we may simply be unable to resolve such structure.[40]

^{14}N ESEEM Spectroscopy. As in the analysis of the hydrogen ESEEM, we focus on spectra derived from the α complex; similar results were obtained for both complexes. Combining frequency tracking and field sampling at the "perpendicular" excitation positions B–D of Figure 1, we identified characteristic features in these orientation-restricted powder spectra, verified their assignment to ^{14}N, and established the nature of each peak within the ^{14}N energy level scheme.[41] From the external field dependence of the ESEEM frequencies we estimate the size of the hyperfine coupling to be ~6.7 (0.1) MHz (~6.5 (0.1) MHz for the β complex).[37] From this estimate we can identify all of the features in the ESEEM spectra. With reference to the dead time reconstructed, cosine-transform spectrum of Figure 2, which we reproduce on an expanded scale in Figure 5, we assign the very weak, broad feature in the neighborhood of 11.5 MHz (and beyond to ~14 MHz, not depicted in the figure) to the sum combination of the fundamental double-quantum frequencies, the peak at 9 MHz to the higher frequency partner[42] of this fundamental pair, and the counterphase peak at 6.7 MHz to the sum combination of the single quantum fundamentals. The spectral intensity at ~5 MHz is comprised of several overlapping elements: the lower frequency double-quantum peak, the double-quantum difference combination, and the higher frequency single-quantum fundamental. The lower frequency partner of the latter contributes to the structured feature at 2 MHz.

We also surveyed the field dependence of ^{14}N ESEEM frequencies under conditions of complete orientation selection (excitation at positions A and E in Figure 1). The signal to noise ratios of the electron spin echoes obtained with parallel versus perpendicular excitation are reduced by 1 order of magnitude, but the overall modulation depths are similar. The dominant spectral features observed again derive from the double-quantum peaks—specifically, the higher frequency fundamental and the difference combination. By tracking the field dependence of the fundamental partner frequencies determined by these two features, we substantiate our assignment of the spectral features and determine the absolute value of the ^{14}N secular hyperfine interaction to be 7.10 (0.05) MHz, while the total, nonsecular contribution[23] is found to amount, in absolute value, to 0.8 (0.1) MHz.[37] Inasmuch as the quadrupolar contribution to the latter is likely to be of order 1, we suspect that nonsecular portion of the hyperfine interaction is small.

Hyperfine couplings of ~7 MHz with ^{14}N have been reported in a number of VO^{2+} complexes with nitrogen donor ligands coordinated cis to the oxo group.[43-50] Moreover, the ESEEM patterns and corresponding spectra obtained by Eaton et al.[47] for

(39) Mims, W. B.; Davis, J. L.; Peisach, J. *J. Magn. Reson.* **1990**, *86*, 273.

(40) Dikanov et al. [Dikanov, S. A.; Evelo, R. G.; Hoff, A. J.; Tyrsyshkin, A. M. *Chem. Phys. Lett.* **1989**, *154*, 34] resolved a splitting in the fundamental ^2H ESEEM peaks in spectra of a number of vanadyl complexes with transligated alcohols. A splitting of a ^2H Larmor peak was also observed in: Mims, W. B.; Peisach, J. *J. Biol. Chem.* **1984**, *259*, 2704.

(41) In many circumstances, the dependence of an ESEEM peak frequency ν, may, to a good approximation, be cast in the form $\nu^2/p^2 - \nu_n^2 = c_1\nu_n + c_0$, in which p indexes the "order" of the surveyed frequency component (single-, double-quantum, etc.), c_1 encompasses the contributions to the ESEEM frequencies of secular interactions (hyperfine interactions only, for the ^{14}N double-quantum peaks), and c_0 incorporates the squares of the secular and nonsecular interactions. Frequency tracking may therefore be utilized to verify the assignment of a peak to a certain nucleus (through ν_n), to a particular set of levels within the nuclear spin energy level scheme (through p), and to quantify spin couplings (from c_1 and c_0, as detailed in refs 19–25).

(42) The "partners" comprise one double-quantum peak from each of the two M_S-indexed manifolds of I.

(43) AStashkin, A. V.; Dikanov, S. A.; Tsvetkov, Yu. D. *Zh. Strukt. Khim.* **1985**, *5*, 53.

(44) (a) de Boer, E.; Keijzers, C. P.; Klaassen, A. A. K.; Reijerse, E. J.; Collison, D.; Garner, C. D.; Wever, R. *FEBS Lett.* **1988**, *235*, 93. (b) Reijerse, E. J.; Shane, J.; de Boer, E.; Collison, D. In *Electron Magnetic Resonance of Disordered Systems*; Yordanov, N., Ed.; World Scientific: Singapore City, 1989; p 1.

(45) Tipton, P. A.; McCracken, J.; Cornelius, J. B.; Peisach, J. *Biochemistry* **1989**, *28*, 5270.

(46) LoBrutto, R. Personal communication.

(47) Eaton, S. S.; Dubach, D.; Kundalika, M. M.; Eaton, G. R.; Thurman, G.; Ambruso, D. R. *J. Biol. Chem.* **1989**, *264*, 4776.

(48) Kirste, B.; van Willigen, H. *J. Phys. Chem.* **1982**, *86*, 2743.

(49) Mulks, C. F.; Kirste, B.; van Willigen, H. *J. Am. Chem. Soc.* **1982**, *104*, 5906.

(50) Mulks, C. F.; van Willigen, H. *J. Phys. Chem.* **1981**, *85*, 1220.

a vanadyl complex of lactoferrin and for an imidazole complex of VO–bis(hexafluoroacetylacetonate) bear a striking similarity to those reported here. This similarity suggests that the ^{14}N ESEEM of VO^{2+}–apoferritin likely stems from coordinated imidazole of a histidine residue rather than some other N donor in the protein. While this suggestion cannot be conclusively confirmed by the spectroscopic results presented here, the combination of these results with the results of prior EPR[3-5] and crystallographic[14] studies—as detailed in the Discussion—further implicates imidazole coordination.

A distinguishing feature of the ^{14}N ESEEM spectra is the broadening of the double-quantum fundamentals and the single-quantum sum-combination peak in excess of widths imposed by the echo decay time. We have outlined[23,25] and will further detail elsewhere[51] both the role that hyperfine anisotropy can play in the (secular) broadening of these peaks and the spectroscopic information that this broadening reveals (hyperfine anisotropy) and conceals (quadrupole interaction): The obscuring of the quadrupolar shift of the double-quantum peaks by nonsecular hyperfine interactions limits our present ability to determine the quadrupole couplings and to employ them to test more critically our assignment of the ^{14}N ESEEM to the nitrogen donor of an imidazole ligand.

We note that, in a VO^{2+}–imidazole complex, the presence of (slightly) inequivalent (coordinated and remote) ^{14}N nuclei can provide an alternative explanation of the excessive line widths. Peaks in ENDOR spectra of vanadyl complexes of imidazole and carnosine have been assigned to both the ligated and remote nitrogens of the imidazole ring—with *both* nitrogens sustaining hyperfine interactions of approximately equal magnitude;[49] ENDOR spectra of VO^{2+} complexes of apoferritin and transferrin show multiple lines that can be attributed to at least two slightly inequivalent nitrogens with coupling constants near 7 MHz.[6] Absent an unusually gross disparity in the quadrupole coupling constants of the two nitrogens, both should contribute to the ESEEM pattern. The amplitudes of the ^{14}N modulations in the VO^{2+} complex of apoferritin are, however, difficult to reconcile with the presence of more than a single nitrogen, unless—contrary to the body of evidence that has emerged from EPR studies[2-6,13]—the presence of more than a single, significantly occupied binding site is assumed. Clearly, additional study and analysis of ESEEM in VO^{2+}–imidazole and other model compounds are warranted to elucidate the nature of vanadyl–^{14}N spin couplings.[52]

IV. Discussion

ESEEM spectroscopy of VO^{2+} complexes of apoferritin provides new insight into the vanadyl binding site not elucidated in previous studies.[2-5] The ESEEM results reveal the presence of a strongly coupled hydrogen located very nearly within the perpendicular plane of the complex, approximately 2.6 Å from the vanadium center. At such a position, this hydrogen is almost certainly attached to a vanadium-coordinated atom that is situated cis with respect to the oxo ligand. Comparison of samples prepared in ^1H_2O and in ^2H_2O establishes the solvent exchangeability of the strongly coupled hydrogen. The vanadyl spin probe is thus accessible to solvent and, by inference, to molecular oxygen—a requirement for a site to be involved in the oxidative deposition of iron in the protein. It seems likely that the binding site for which VO^{2+}, Fe^{2+}, and Fe^{3+} compete in horse spleen apoferritin, and from which the Fe^{3+} complex is obtained upon oxidation of Fe^{2+}, promotes initial iron oxidation in the protein and, as suggested below, may facilitate the hydrolysis and polymerization reactions that ultimately lead to core formation.

The marked pH dependence of the EPR spectrum of the VO^{2+}–apoferritin complex is of special interest because of its possible significance to the mechanism of iron deposition. The only substantial distinction between the ESEEM spectra of the α and β complexes is the reduction in amplitude of the modulation from the strongly coupled hydrogen: The ESEEM amplitudes indicate that the number of such hydrogens is one to two in the α complex and roughly half this number in the β complex (Figure 3). These results are readily accommodated by the proposal[5] that deprotonation of an aquo ligand underlies the difference between the EPR spectra of the α and β complexes. This idea is appealing because of the well-known tendency of VO^{2+} complexes (as well as Fe^{3+} complexes) to undergo hydrolysis reactions. For example, vanadyl complexes of iminodiacetate and nitrilotriacetate, which are reasonable models for the VO^{2+}–apoferritin complex (vide infra), have hydrolysis pK_a values of 5.8 and 7.2, respectively.[55] These values bracket the apparent pK_a 6.5 observed in VO^{2+}–apoferritin—that is, the pH at which the EPR signals of the α and β species have equal intensity.[5] Moreover, the change in the values of the EPR parameters associated with the α to β conversion is in accord with ligand additivity relationships for the change of one H_2O into an OH^- ligand.[13] Such a change, in the case of the Fe^{3+}–protein complex, is expected to be the first step in the sequence of hydrolysis–polymerization reactions through which the mineral core is formed. Both Fe^{3+} and VO^{2+} are well-known to form polymeric hydrous oxide species at elevated pH.[11,12] The coordination of water at the VO^{2+} binding site makes the site well suited for facilitating hydrolysis reactions which can lead to core formation.

We reiterate the special utility of the combination frequencies inherent in two-pulse ESEEM spectra[16] in identifying the strongly coupled proton. The large line width associated with the fundamental frequency peaks of nuclei that sustain a large dipolar interaction is effectively canceled in the sum-combination peak, thus enabling its observation by ESEEM spectroscopy. Furthermore, the frequency shift of the sum-combination peak is predominantly governed by the dipolar rather than the isotropic hyperfine coupling. Accordingly, difficulties in the spectroscopic characterization of metal binding sites posed by heterogeneity in the isotropic couplings are circumvented by this ESEEM method. The broadening associated with such heterogeneity can limit sensitivity in proton ENDOR spectroscopy.[53] The analysis of the combination frequencies in two-pulse ESEEM spectra should have applicability to the study of metal ion coordination in a variety of metal–protein complexes.

The ESEEM results establish the presence of endogenous nitrogen in the vicinity of VO^{2+} in apoferritin (Figures 2 and 5); this finding is in accord with recent ENDOR results.[6] The observed nitrogen modulations are best interpreted as arising from the nitrogens of a cis-coordinated imidazole of a histidine residue: The ^{14}N hyperfine coupling constants for VO^{2+}–apoferritin are very similar to those reported elsewhere for vanadyl chelate and protein complexes with cis-coordinated nitrogen.[43-50] Furthermore, detailed similarities exist between the ESEEM patterns and spectra reported here and those found by Eaton et al. for VO^{2+} coordinated by a single imidazole.[47] Finally, in horse spleen apoferritin crystals grown in solutions of $CdSO_4$, histidine is the only N donor ligand found at any of the binding sites of Cd^{2+},[14] which competitively displaces VO^{2+} in apoferritin.[4,5]

Taken jointly, the EPR[4,5] and ESEEM results reflect a single, dominant type of binding site with carboxylate, histidine, and aquo ligands.[56] Recent ENDOR results are consistent with this view and, moreover, demonstrate the interrelationship of the vanadyl

(51) Cosgrove, S. A.; Gerfen, G. J.; Singel, D. J. Unpublished results.
(52) Further discussion and quantitative analysis of the ^{14}N ESEEM may be found in ref 25.
(53) Orientation-selective excitation can overcome in analogous fashion the dipolar broadening of the proton ENDOR lines. It is interesting to note, however, that in $VO(H_2O)_5^{2+}$ (see ref 31) the ENDOR lines obtained with parallel excitation for protons attached to the cis aquo ligands are not resolved from ENDOR of the "matrix" protons.
(54) SDS gel electrophoresis shows that ~96% of the subunits of the horse spleen apoferritin used in this work are of the L-chain, rather than H-chain, variety. The residues of the H-chain ferroxidase site are not conserved in the L-chain but are altered to Tyr, Phe, and Gly, respectively (see ref 1c).
(55) Smith, R. M.; Martell, A. E. *Critical Stability Constants, Vol. 6: Second Supplement*; Plenum: New York, 1989; pp 68 and 77.
(56) Inasmuch as apoferritin is known to have many different sites for metal ions (see ref 14), the possibility that the strongly coupled proton and the nitrogen modulations derive from different vanadyl sites—perhaps involving a minority site not distinguished in the EPR spectrum—cannot be positively ruled out.

binding sites with iron sites where bound Fe^{2+} is perhaps oxidized to bound Fe^{3+}.[6] This ligand set is wholly consistent, by ligand additivity criteria,[13] with the EPR parameters of VO^{2+}–apoferritin[4,5] and forms a site well suited for binding both Fe^{2+} and Fe^{3+}. Recent work has shown the presence of a metal binding site in the H-chain subunit of human apoferritin that is the locus of activity for iron oxidation. This site is comprised of the side chains of Glu 27, His 65, and Glu 62, together with an aquo ligand.[10] Although the paucity of H-chain subunits in the equine protein[54] precludes this site from being the dominant binding site of VO^{2+} in horse spleen apoferritin, it is nevertheless interesting to note the correspondence in chemical composition of this ferroxidase active site with the VO^{2+} site characterized here by ESEEM.

The metal ion (specifically, Cd^{2+}) complex with horse spleen apoferritin that has been shown by X-ray crystallography[14] to be comprised, in part, of N donor and carboxylate ligands is located on the interior of the protein coat near the hydrophilic channels. The side chains of His 132 and Asp 135′[57] are components of the site. Three sites, associated with the set of three protein subunits related by the symmetry axes that lie along the channels, are situated near each channel. In light of the stoichiometry of VO^{2+} binding to apoferritin,[4] the results of metal ion binding competition studies,[4-6] and structural information drawn from EPR,[4,5] ENDOR,[6] and ESEEM spectroscopy, it is tempting to identify this interior site as the principal VO^{2+} binding site in apoferritin. Details of the mode of VO^{2+} uptake by apoferritin—the saturation of the binding capacity at 16 vanadyl equivalents per (24-subunit) protein, the reduced affinity of the protein for the second set of eight vanadyl ions bound as compared to the first set, and the EPR equivalence of all ions bound—are also readily accommodated within this model, provided some negative cooperativity in binding is assumed to operate among the sites associated with each channel in the regulation of metal ion uptake. This hint of cooperative behavior among symmetry-related metal ion binding sites may have intriguing ramifications for the chemistry of apoferritin.

Acknowledgment. This work was supported by NIH Grants GM20194 (N.D.C.) and GM07598 (G.J.G.) and by the John L. Loeb Foundation (D.J.S.).

Appendix

Comments on the Analysis of the Frequency Shift of the Proton Sum-Combination Peak. Direct use of eq 1 to evaluate A_2^0 from the measured value of $(2\nu_p\Delta\nu)^{1/2}$ is not strictly justified if the microwave excitation is orientationally selective to any significant degree. Orientationally selective excitation can lead to a reduction in both the frequency shift and the amplitude of the shifted ESEEM component. Both vary essentially as a power of sin (2θ), where θ is the (minimum) angle between some uniquely selected orientation and the major axis of the proton hyperfine interaction matrix. Consequently, in the case of parallel excitation of the EPR spectrum, the shift and amplitude would tend toward zero as θ tends either toward 0 or $\pi/2$, that is for protons with major axes aligned either along the parallel axis or within the perpendicular plane. In the case of perpendicular excitation, protons with major axes near the parallel axis would again exhibit small shifts and amplitudes ($\theta \approx \pi/2$); for protons near the perpendicular plane, however, the average over the azimuthal orientations (where θ ranges from ~ 0 to $\pi/2$) could yield large amplitudes and shifts. These qualitative ideas are confirmed in generic ESEEM simulations that we have undertaken. Qualitatively, we note that full frequency shift of eq 1, together with essentially maximal amplitude, is realized in the case of perpendicular excitation, provided only that the angle between the hyperfine major axis and the normal to the (perpendicular) plane of excitation exceeds $\sim\pi/4$.

An additional factor that exerts a weak influence on the shift is the isotropic hyperfine interaction A_0^0.[33,34] (Equation 1 applies in the limit $A_0^0/\nu_p \to 0$.) Our generic simulations indicate that nonzero values of A_0^0 tend to *increase* the shift slightly. This tendency is graphically illustrated in ref 33. More specifically, our simulations show that, for $\nu_p \sim 12.59$ MHz and $A_2^0 = 4.2$ MHz, a value for A_0^0 of 9 MHz (vs 0 MHz)—the largest value observed by Atherton and Shackelton[29]—increases the shift by $\sim$30%. Failure to take the isotropic coupling into account in the analysis of shifts encountered in this instance would lead to a small ($\sim$5%) underestimate of the V–H distance.

With these factors in mind, our ^1H ESEEM data enable us to conclude that the shifted peak must derive from protons attached to the coordinated atom of a cis ligand. We first note that the size of the observed shifts indicates that the relevant protons must lie within a few angstroms of the vanadyl ion and are therefore certainly attached to atoms coordinated to the metal ion.

The absence of a shifted sum-combination peak in spectra obtained with parallel excitation (or of the corresponding fundamentals, which should be narrowed by complete orientation selection) is understandable as a joint consequence of orientation selectivity and ESEEM amplitude anisotropy, provided the proton hyperfine major axis is nearly coincident with ($\theta \approx 0$) or orthogonal to ($\theta \approx \pi/2$) the parallel orientation. This arrangement would be realized for protons attached to ligated atoms if the parallel orientation is nearly aligned with the V–O bond direction: θ would be ~ 0.4–0.5π for a proton attached to a cis-ligated atom and in the range -0.1π to $+0.1\pi$ for a trans ligand. The near-coincidence of the parallel orientation—that is, the common (unique) principal axes of the electron **g** and ^{51}V hyperfine matrices—with the V–O bond direction is typical in vanadyl complexes.[13]

The sum-combination splittings observed in spectra obtained with perpendicular excitation indicate that the coordination position of the atom in question must be cis rather than trans. First, if the relevant proton were attached to a trans-ligated atom, we would anticipate an ESEEM amplitude that is attenuated by orientation-selection effects to an extent similar to that attending parallel excitation. Our observation of a shifted sum-combination peak of substantial amplitude argues against trans location. Furthermore, in the case of trans ligation, the actual dipolar coupling would have to be greater than the observed value of $(2\nu_p\Delta\nu)^{1/2}$ (approximately 5.0 MHz based on our generic simulations) because of orientation selection effects. Such a value is grossly different from the pertinent value (3.3 MHz) of Atherton and Shackleton;[29] it implies a V–H distance less than 2.53 Å—a value untenably short for a trans ligand. The introduction of a large value for A_0^0 could, in principle, alleviate this discrepancy, but such a value is intrinsically inconsistent with the hypothetical trans location of the ligand. The alternative, attachment to a cis-ligated atom, leads to a gratifying reconciliation with the ENDOR results.[29] In this situation, the actual dipolar coupling can be equated with $(2\nu_p\Delta\nu)^{1/2}$ (or a somewhat reduced value, vide supra, if the isotropic coupling is large). The observed value of $(2\nu_p\Delta\nu)^{1/2}$, namely 4.34 MHz (α complex), accords extremely well with the cited ENDOR results[29] and also implies a very reasonable V–H distance of 2.64 Å.

(57) The prime designates an adjacent subunit.